















RESEARCH ARTICLE

Acute inhibition of AMPA receptors by perampanel reduces amyloid β -protein levels by suppressing β -cleavage of APP in Alzheimer's disease models

Sakiho Ueda¹  | Akira Kuzuya¹  | Masayoshi Kawata²  | Kohei Okawa¹  |
Chika Honjo¹  | Takafumi Wada¹  | Mizuki Matsumoto¹  | Kazuya Goto³  |
Masakazu Miyamoto¹  | Atsushi Yonezawa²  | Yasuto Tanabe³  | Akio Ikeda⁴  |
Ayae Kinoshita⁵  | Ryosuke Takahashi¹ 

¹Department of Neurology, Graduate School of Medicine, Kyoto University, Kyoto, Japan

²Department of Clinical Pharmacology and Therapeutics, Kyoto University Hospital, Kyoto, Japan

³Department of Regulation of Neurocognitive Disorders, Graduate School of Medicine, Kyoto University, Kyoto, Japan

⁴Department of Epilepsy, Movement Disorders and Physiology, Graduate School of Medicine, Kyoto University, Kyoto, Japan

⁵School of Human Health Sciences, Faculty of Medicine, Kyoto University, Kyoto, Japan

Correspondence

Akira Kuzuya, Department of Neurology, Graduate School of Medicine, Kyoto University, 54 Shogoin Kawahara-Cho, Sakyo-Ku, Kyoto 606-8507, Japan.

Email: akuzuya@kuhp.kyoto-u.ac.jp

Funding information

MEXT | Japan Society for the Promotion of Science (JSPS), Grant/Award Number: JP21K20690 and JP20K07884

Abstract

Hippocampal hyperexcitability is a promising therapeutic target to prevent A β deposition in AD since enhanced neuronal activity promotes presynaptic A β production and release. This article highlights the potential application of perampanel (PER), an AMPA receptor (AMPA) antagonist approved for partial seizures, as a therapeutic agent for AD. Using transgenic AD mice combined with in vivo brain microdialysis and primary neurons under oligomeric A β -evoked neuronal hyperexcitability, the acute effects of PER on A β metabolism were investigated. A single oral administration of PER rapidly decreased ISF A β_{40} and A β_{42} levels in the hippocampus of J20, APP transgenic mice, without affecting the A β_{40} /A β_{42} ratio; 5 mg/kg PER resulted in declines of 20% and 31%, respectively. Moreover, PER-treated J20 manifested a marked decrease in hippocampal APP β CTF levels with increased FL-APP levels. Consistently, acute treatment of PER reduced sAPP β levels, a direct byproduct of β -cleavage of APP, released to the medium in primary neuronal cultures under oligomeric A β -induced neuronal hyperexcitability. To further evaluate the effect of PER on ISF A β clearance, a γ -secretase inhibitor was administered to J20 1 h after PER treatment. PER did not influence the elimination of ISF A β , indicating that the acute effect of PER is predominantly on A β production. In conclusion, acute treatment of PER reduces A β production by suppressing β -cleavage of amyloid- β precursor protein effectively, indicating a potential effect of PER against A β pathology in AD.

KEYWORDS

Alzheimer's disease, amyloid β -protein, in vivo microdialysis, perampanel, β -Cleavage of APP

Abbreviations: aCSF, artificial cerebrospinal fluid; AD, Alzheimer's disease; AED, antiepileptic drug; AMPAR, α -amino-3-hydroxy-5-methyl-4-isoxazole propionic acid receptor; APP, amyloid- β precursor protein; A β , amyloid β -protein; A β O, oligomeric A β ; FL-APP, full-length APP; ISF, interstitial fluid; PER, perampanel; sAPP α , soluble APP α ; sAPP β , soluble APP β ; SNS, synaptoneurosome; TH, total homogenate; α CTF, α -secretase-cleaved C-terminal fragment of APP; β CTF, β -secretase-cleaved C-terminal fragment of APP.

This is an open access article under the terms of the [Creative Commons Attribution](https://creativecommons.org/licenses/by/4.0/) License, which permits use, distribution and reproduction in any medium, provided the original work is properly cited.

© 2023 The Authors. *The FASEB Journal* published by Wiley Periodicals LLC on behalf of Federation of American Societies for Experimental Biology.

1 | INTRODUCTION

Alzheimer's disease (AD) is a multifactorial neurodegenerative disorder, with several mechanisms contributing to its etiology. The key initiator of AD pathogenesis is amyloid β -protein ($A\beta$).¹ The $A\beta$ cascade hypothesis suggests that $A\beta$ aggregation plays a pivotal role in the pathological cascade of AD, leading to the formation of amyloid plaques, neurofibrillary tangles, and ultimately neurodegeneration.² This hypothesis has guided the development of various therapeutic strategies targeting $A\beta$ to mitigate disease pathogenesis and progression. $A\beta$ is derived from the sequential proteolytic cleavage of amyloid- β precursor protein (APP) by β - and γ -secretases.^{3,4} The causal mutations identified in familial AD are located in the gene encoding presenilin or APP, leading to increased $A\beta$ production and aggregation. Additionally, a rare protective mutation against sporadic AD, an APP A673T variant, has been reported to decrease $A\beta$ burden in the brain and preserve cognitive functions, leading further support to the $A\beta$ cascade hypothesis.⁵

Recent studies shed light on hippocampal network hyperexcitability as an early event in the pathophysiology of AD. It has been clinically well known that, in patients with AD, the comorbidity of epilepsy is common, with rates reaching to 30%–60% in familial AD patients and 10%–22% in sporadic ones.^{6–10} Detailed studies using electroencephalography (EEG) revealed a higher prevalence of epileptiform activity in early AD patients that was profoundly associated with the onset or progression of cognitive decline than expected.^{11,12} As silent hippocampal seizures and epileptiform spikes were detected by using only intracranial electrodes placed adjacent to the mesial temporal lobe (called foramen ovale electrode) in two AD patients without a history of epilepsy,¹³ it could be one reasonable explanation for the occult epileptiform activity that, in early AD patients, neuronal hyperexcitability can locally occur in the hippocampus where epileptiform discharges are challenging to be detected on routine scalp EEG. Intriguingly, comorbid epilepsy in AD patients even without clinical seizures markedly promotes cognitive decline,^{11,12} and several studies reported that low-dose levetiracetam (LEV), a newer antiepileptic drug (AED) targeting the synaptic vesicle glycoprotein 2A (SV2A), has an effect on cognitive function in patients with mild cognitive impairment or AD.^{14–16} However, AEDs may be inappropriate for AD under certain conditions. Some AEDs and high-dose LEV were ineffective in improving cognitive function, and phenytoin and pregabalin aggravated epileptic discharges in an AD mouse model.^{17,18} Further, multiple AEDs reportedly can deteriorate various cognitive disorders in a type and/or dose-dependent fashion,^{19–26} suggesting the importance of determining the

appropriate type and dose of AED in view of therapeutic development against AD based on the “neuronal hyperexcitability hypothesis.”

A decline of synaptic α -amino-3-hydroxy-5-methyl-4-isoxazole propionic acid receptors (AMPA) and a suppression of long-term potentiation (LTP) are the earliest well-established changes observed in AD.^{27–29} However, as early as these findings, excessive glutamate-mediated stimulation of N-methyl-D-aspartate receptors (NMDARs) and AMPARs is considered to induce excitotoxicity in a calcium-dependent pathway under AD pathophysiology.^{30–33} While AMPARs predominantly mediate the fast excitatory transmission in the brain, direct stimulation with AMPA increases non-amyloidogenic processing of APP and inhibits $A\beta$ production in wild-type primary neurons. Sustained stimulation with AMPA also promotes $A\beta$ clearance in APP-transgenic mice.³⁴ However, few reports have investigated how suppressing excessive AMPAR excitability affects $A\beta$ metabolism. In the present study, we focused on perampanel (PER), a selective noncompetitive AMPAR antagonist, as a potential therapeutic agent against AD.^{35,36} Excitatory neurons upregulating AMPARs contribute substantially to epileptogenicity, and a low inhibition of AMPARs is sufficient for seizure protection in patients with epilepsy,^{37–40} supporting the outstanding contribution of AMPAR in generating epileptogenicity. The previous study has shown that AMPAR modulation by PER reduces neuronal hyperactivity and synchronization while it does not affect physiological synaptic transmission.⁴¹

PER is well tolerated in elderly people aged ≥ 65 years, whereas low-dose PER showed high efficacy in treating elderly-onset epilepsy concomitant with AD.^{42,43} Surprisingly, they also described that in 80% of 48 patients, conventional-dose PER improved cognitive function and seizure control (reported in Japanese).⁴⁴ The narrow-spectrum AED targeting only excitatory neurons could be appropriate for suppressing aberrant neuronal activities without inhibiting regular neuronal transmission. However, reports on the use of PER in AD patients are limited, and a potential effect of PER on AD pathophysiology has not yet been fully elucidated at the molecular levels. In the present study, we aimed to investigate whether the acute treatment of PER could affect hippocampal $A\beta$ metabolism in APP transgenic mice using an in vivo brain microdialysis technique.

2 | MATERIALS AND METHODS

2.1 | Animals

All procedures were approved by the Institutional Animal Care Committee of the Kyoto University Graduate

School of Medicine in accordance with the guidelines for animal experimentation from the ethical committee of Kyoto University and with the National Research Council's Guide for the Care and Use of Laboratory Animals. We used PDGFB-APPSwInd transgenic (Tg) mice (J20) expressing a mutant form of the human APP bearing both the Swedish (K670N/M671L) and Indiana (V717F) mutations (APP_{Sw/Ind}) under the control of the PDGFB promoter in a C57BL/6J (B6) genetic background (Jackson Laboratory) as an AD model and the littermates as a control. All animals were derived from the same colony. Altogether, 52 J20 mice (2–4-month-old; $n = 45$, 9–11-month-old; $n = 7$) were implanted with microdialysis probes; B6 ($n = 6$) and J20 ($n = 4$) mice were used for the blood test; and J20 ($n = 21$) and B6 ($n = 1$) mice were used for the biochemical analysis of the hippocampus and synaptoneuroosomes (SNSs). ICR mice were purchased from Shimizu Laboratory (Kyoto, Japan) to perform cortical primary neuronal cultures.

2.2 | Compounds

Perampanel (PER; Eisai Co., Tokyo, Japan) was diluted in DMSO, PEG300, and double distilled water (1:1:1) to 0.5 and 0.2 mg/mL for the 5 and 2 mg/kg PER administrations, respectively. LY411575 (Sigma-Aldrich, St. Louis, USA), a potent γ -secretase inhibitor, was diluted in dimethyl sulfoxide (DMSO) and polyethylene-glycol (PEG) 300 (1:2) to 1 mg/mL. Tetrodotoxin (TTX; Nacalai tesque, Kyoto, Japan) was diluted to 2 mM with 14 mM HCL. L-glutamic acid (Nacalai tesque, Kyoto, Japan) was dissolved in the medium to a concentration of 1 mg/mL.

2.3 | Preparation of A β oligomers

Monomeric A β_{42} was synthesized from the O-acyl isopeptide (Peptide Institute, Osaka, Japan). The O-acyl isopeptide was diluted with 14 mM of HCl to a concentration of 30 μ M and neutralized with 30 mM of NaOH. The medium was added to achieve a final concentration of A β_{42} of 20 μ M. The adjusted monomeric A β_{42} was incubated at 37°C for 48 h to obtain oligomeric A β (A β O). The A β O solution was used in experiments immediately after preparation.

2.4 | Primary cultures of mouse cortical neurons and induction of A β O-evoked neuronal hyperexcitability

Primary neuronal cultures were obtained from 15-day-old embryos of wild-type ICR mice. Cortical neurons were

extracted using a Papain Dissociation System (Worthington Biochemical Corporation, NZ, USA) and plated onto tissue culture 6 well plates (Gibco, WA, USA) coated with polyethylene imine at a density of 6×10^6 . Cells were cultured for 28 days in vitro (DIV) in Neurobasal™ Plus Medium with B-27 Plus Supplement (Gibco, MA, USA) and a 1% penicillin–streptomycin solution mixture in a 37°C, 5% CO₂ incubator. To establish A β O-evoked neuronal hyperexcitability as in an vitro AD model, 0.5 μ M A β O and 1 μ M TTX were simultaneously applied to primary neuronal cultures at 28 DIV for 24 h, according to a previous report.⁴⁵ Subsequently, the culture media were treated with fresh media containing 30 μ M L-glutamic acid, and either 2 μ M PER or the vehicle were replaced after a gentle wash with PBS. After 70 min, the conditioned media were collected, and the neuronal cells were harvested for biochemical analysis.

2.5 | In vivo A β microdialysis

For the continuous interstitial fluid (ISF) collection, we used an in vivo microdialysis technique, as described previously. J20 mice were anesthetized with isoflurane, and guide cannulas (BR Intracerebral Guide Cannula; BASi, Indiana, USA) were stereotaxically implanted above the left hippocampus (bregma -3.1 mm, 2.5 mm lateral to the midline, and 1.2 mm ventral to dura at a 12° angle). The cannulas were mounted with dental cement. One day after the implantation of the guide cannulas, microdialysis probes (BR-2 2 mm 38 kDa MWCO polyacrylonitrile membrane, BASi) were inserted into the hippocampus through the guide cannula while perfused with artificial cerebrospinal fluid (aCSF: 122 mM NaCl, 1.3 mM CaCl₂, 1.2 mM MgSO₄, 3.0 mM KCL, 4 mM KH₂PO₄, and 25 mM NaHCO₃, pH 7.35) with 0.15% bovine serum albumin (BSA; Sigma-Aldrich) at a rate of 1.0 μ L/min for 13 h before starting the sampling ISF. The samples were maintained at 4°C in a fraction collection and stored until analysis at -80°C . After sampling ISF, animals were perfused with 0.2% Evans blue in aCSF for 90 min, and the brains were rapidly detected to confirm the accuracy of probe insertion into the hippocampus.

Using the in vivo microdialysis technique described above, hippocampal ISF was collected from young J20 (2–4-month-old; $n = 7$, male 4, female 3) and old (9–11-month-old; $n = 7$, male 4, female 3) mice to determine the A β_{40} and A β_{42} levels. The average hippocampal ISF A β_{40} and A β_{42} levels and the ratio of A β_{40} /A β_{42} were plotted during the 270-min steady-state after the 13-hour preperfusion.

While sampling hippocampal ISF every 90 min, J20 mice (2–4-month-old; $n = 10$, male 5, female 5) were orally administered with either PER (2 and 5 mg/kg) or vehicle using flexible plastic feeding tubes after the basal sampling

of ISF for three-time points during 270 min. ISF was collected at 12 h after the treatment. The values of either ISF A β_{40} or A β_{42} were plotted as the percentage to the basal levels and A β_{40} /A β_{42} ratio.

2.6 | ISF A β elimination half-life

J20 mice (2–4-month-old; $n=4$) were injected with LY411575 subcutaneously at a dose of 3 mg/kg at 1 h after the oral gavage of 5 mg/kg PER, while hippocampal ISF was collected every 60 min. ISF was collected at 6 h after administering LY411575. ISF A β_{40} levels were plotted as the percentage to those at a time point before the treatment. The elimination half-life of A β_{40} was calculated from the slope of the ISF levels and time curve by plotting on a semilogarithmic graph.⁴⁶

2.7 | Hippocampal homogenates after acute administration of PER

The brain of J20 mice was rapidly dissected at 5 h after the oral administration of PER (5 mg/kg) ($n=5$, male 3, female 2) or vehicle ($n=5$, male 2, female 3). The isolated hippocampi were homogenized in 10% (w/v) Tris-buffered saline (50 mM Tris-HCl, 150 mM NaCl, pH 7.6) with 1% (v/v) protease and phosphatase inhibitor cocktail (PPI) (Thermo Fisher Scientific, MA, USA) and sonicated by Biorupter (Cosmo Bio, Tokyo, Japan) for 30 sec followed by ultracentrifugation at 100 000 \times g for 45 min at 4°C in an angle rotor (OPTIMA max TLA-55; Beckman Coulter, Brea, Cal). The pellets were resuspended in RIPA buffer (50 mM Tris-HCl, 0.15 M NaCl, 0.1% (w/v) SDS, 1% (v/v) Triton X-100, 10% (v/v) sodium deoxycholate) with 1% (v/v) PPI and ultracentrifuged at 100 000 \times g for 45 min at 4°C in an angle rotor. The supernatant was stored until analysis at -80°C as the hippocampal homogenates.

2.8 | Isolation of synaptoneuroosomes (SNSs) from the hemicortex dissected after PER administration

SNSs were isolated as described previously^{47,48} with minor modifications. The brains were rapidly collected from J20 mice sacrificed at 5 h after the oral administration of 5 mg/kg PER ($n=6$, male 3, female 3) or vehicle ($n=6$, male 3, female 3). Data obtained from a single female mouse in the vehicle group was excluded after analysis because of a genotyping error. The hemicortex was homogenized in the 1.5 mL SNS buffer (25 mM Tris-HCl,

120 mM NaCl, 5 mM KCl, 1 mM MgCl₂, 2 mM CaCl₂, 2 mM DTT, pH 7.5) with 1% (v/v) PPI and disrupted by the Digital Homogenizer HK-1 (ASONE, Osaka, Japan) at 5000 rpm for 10 min. The sample was loaded into a 2 mL leuc-lock syringe (HENKE-Sass Wolf, Tuttlingen, Germany) and filtered through two layers of 80 μm pore nylon filters held in a filter holder (Merk, Darmstadt, Hessen, Germany). The 100 μL filtrate was diluted in 100 μL DDW with 3% SDS, 4 mM DTT, and 2% (v/v) PPI. The obtained sample was the total homogenate (TH) and was stored at -80°C . The rest filtrate was again loaded into a 2 mL leuc-lock syringe and filtered through a 5 μm pore Supor[®] Membrane (PALL, New York, USA). The filtrate was then centrifuged at 1000 \times g for 10 min. The pellet corresponded to the SNS fraction and was stored at -80°C after the resuspension in 50 mM Tris-HCl buffer with 1.5% (v/v) SDS, 2 mM DDT, and 1% (v/v) PPI.

2.9 | A β ELISA

The ISF samples were diluted three folds and determined by using the Human/Rat β Amyloid⁴⁰ ELISA Kit Wako II #294-64701 (Wako, Tokyo, Japan) for A β_{40} and Human/Rat β Amyloid⁴² ELISA Kit Wako II #292-64501 (Wako) for A β_{42} . The absorbance at 450 nm was measured using a SynergyTMH4 Hybrid Microplate Reader (BioTek, VT, USA).

2.10 | sAPP α and sAPP β ELISA

The levels of endogenous sAPP α and sAPP β in the conditioned media of primary neuronal cultures were quantified by Mouse sAPP α Assay Kit (IBL, Gunma, Japan) and Mouse sAPP β -w Assay Kit (IBL, Gunma, Japan), respectively.

2.11 | BCA assay

The protein quantification of cell lysates of primary neurons and hippocampal homogenates extracted from J20 mice after the oral administration of PER (5 mg/kg) was performed by PierceTM BCA Protein Assay kit (Thermo Fisher Scientific). The absorbance at 562 nm was measured using a SynergyTMH4 Hybrid Microplate Reader.

2.12 | Cell death assay in primary neuronal cultures

To assess cytotoxicity of the cultured primary neurons, the levels of lactate dehydrogenase (LDH) released into

the culture media through compromised cell membranes were measured using a WST assay kit (Dojindo Molecular technologies, Kumamoto, Japan) according to the manufacturer's instructions.

2.13 | Western blotting

The following primary antibodies were used: purified anti- β -amyloid raised against the N-terminus^{1–16} of human A β (6E10 antibody, 1:2000, #9320, Biolegend, CA, USA); anti-APP raised against the C-terminus (1:2000, Sigma-Aldrich, St. Louis, U.S.A.); anti-BACE1 raised against the N-terminus^{46–62} (1:2000, Sigma-Aldrich, St. Louis, U.S.A.); anti-Synaptotagmin 1 (Syt1) raised against the C-terminus (1:500, Merk); anti- postsynaptic density protein 95 (PSD95) (1:1000, D27E11, Cell Signaling Technology, Massachusetts, USA); anti-GluA1 (1:200, C3T, Merck); anti-GluA2 (1:200, R&D systems, Minnesota, USA); and anti- β -actin (1:3000, MBL, Tokyo, Japan). Horseradish peroxidase (HRP)-conjugated goat antibodies were used as secondary antibodies (1:3000, Jackson Immuno Research, PA, USA).

The samples were diluted with 4 \times LDS sample buffer (Invitrogen, MA, USA) containing 10 \times reducing agent (Invitrogen) and denatured at 95°C for 10 min. The samples at 20 μ g protein levels were applied to 4%–10% NuPAGE Bis-Tris gel NP0335BOX (Thermo Fisher Scientific). After electrophoresis, the proteins were transferred to Novex PVDF membranes (Invitrogen). The target proteins were applied using Chemi-Lumi One Super (Nacalai tesque, Kyoto, Japan) and detected using an ImageQuant LAS500 system (GE Healthcare Bio-Sciences, Uppsala, Sweden). The band intensities were measured using ImageJ (National Institute of Health, USA) and normalized to β -actin.

2.14 | Sample preparation for liquid chromatograph–mass spectrometer (LC–MS)/MS to assess the plasma concentration of PER

Blood samples (80–100 μ L/time point) were collected from the facial vein of B6 mice at 1, 3, 6, and 9 h after the oral gavage of PER at a dose of 2 ($n = 4$, male 2, female 2) or 5 ($n = 4$, male 2, female 2) mg/kg. Blood samples of J20 mice ($n = 4$, male 1, female 3) were collected at 1 and 5 h after the administration of 5 mg/kg PER. The obtained blood samples were immediately centrifuged at 12 000 rpm for 10 min, and the supernatants were assayed by LC–MS/MS. PER dilution in DMSO (10 mg/mL) was dissolved in methanol to prepare the stock solutions (10 μ g/mL). The standard working solution for the calibration curve was prepared by diluting the

stock solutions with plasma at PER doses of 0, 0.005, 0.01, 0.05, 0.1, 0.5, 1, and 1.5 μ g/mL. Twenty-five μ L of the standard working solution or the plasma samples were added with 150 μ L of methanol and centrifuged at 15 500 \times g for 10 min. The supernatants were applied to 0.22 μ m filter units (#SLGV004SL; Merk).

2.15 | LC–MS/MS conditions

The samples were analyzed using a triple quadrupole LC–MS (LC–MS 8040 Shimadzu Corporation, Kyoto, Japan) system on an Acquity UPLC BEH C18 column (1.7 μ m 50 \times 2.1 mm; Waters, Milford, MA, USA), as previously reported with some modifications.⁴⁹ The MS/MS data acquisition was performed under Multiple Reaction Monitoring in positive electrospray ionization mode. The mobile phases comprised eluents A (10 mM ammonium acetate, 0.1% (v/v) formic acid in the water) and B (methanol). The flow rate was 0.4 mL/min and the total run time was 5 min with the following gradient program: 50% eluent B (0 min), 50% (0.5 min), 65% (2 min), 95% (2.1 min), 95% (4 min), and 50% (4.1 min). The total volume was 2 μ L. The ion spray voltage was set at +1000 V. The curtain gas pressures were set at 20 U and the collision gas at medium. The ion source gas pressures were set at 45 and 40 U, with temperatures at 400°C. The precursor/product ion transition for PER was m/z 350.0/219.1.

2.16 | Statistical analysis

The statistical data were calculated using GraphPad Prism 8 software (Dotmatics, Boston, MA, USA). Student's t-test, two-way repeated measure analysis of variance (ANOVA) (with the Greenhouse–Geisser correction and Huynh–Feldt correction) with posthoc-Bonferroni, and analysis of covariance (ANCOVA) were used. All data are shown as means \pm SEM, and the p value <.05 indicated a significant difference.

3 | RESULTS

3.1 | ISF levels of monomeric A β ₄₂ rather than A β ₄₀ are preferentially decreased in old J20 mice with A β deposition

In J20 mice, A β oligomers in the brain significantly elevate by 2–3 months, with plaques appearing after 7 months of age.^{50,51} Our laboratory observations also confirm the presence of A β plaques in J20 mice after 7 months of age.⁵² These mice exhibit synaptotoxicity and neuronal loss prior

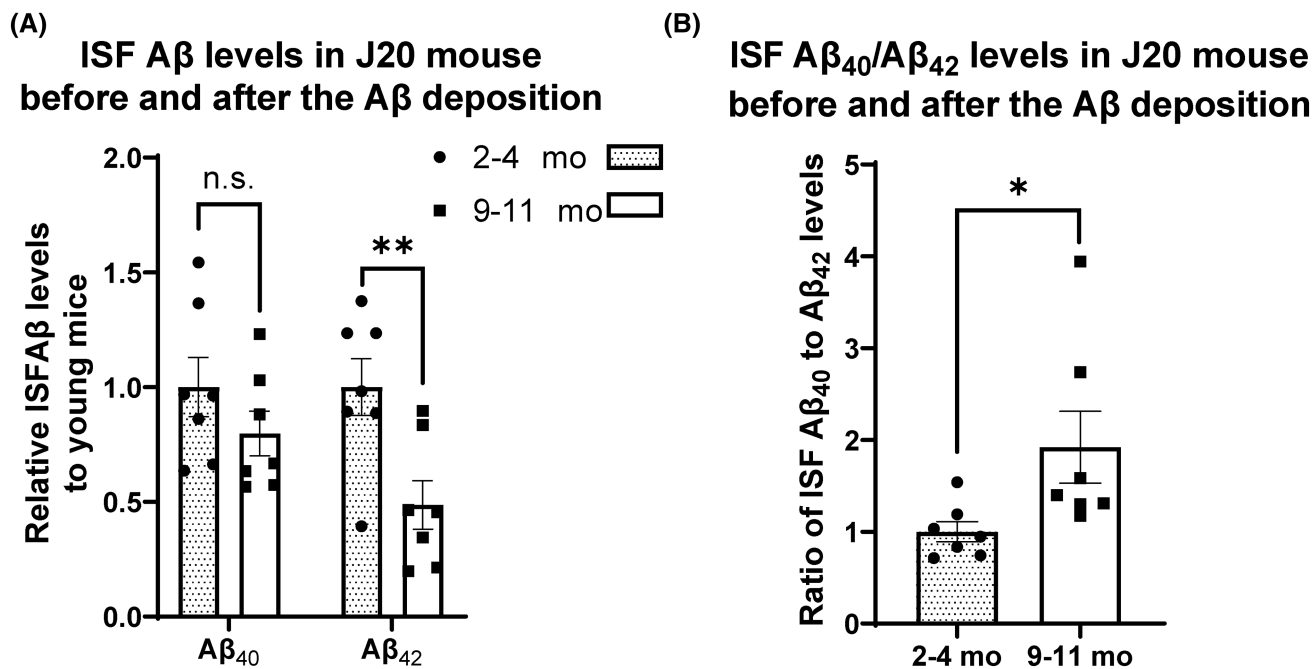


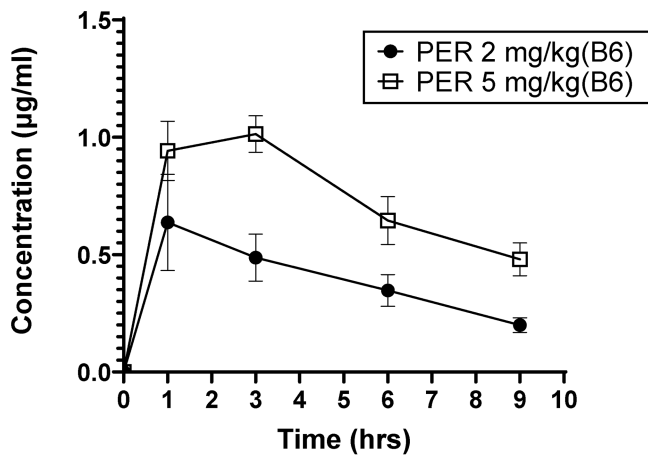
FIGURE 1 ISF Aβ₄₂ levels rather than Aβ₄₀ are preferentially decreased in old APP Tg (J20) mice with Aβ deposition. (A) Average ISF Aβ₄₀ and Aβ₄₂ levels in old J20 mice with Aβ deposition (9–11 months of age, $n = 7$) versus young J20 mice without Aβ deposition (2–4 months of age, $n = 7$) are measured using Aβ ELISA. In the old mice, ISF Aβ₄₂ levels significantly decreased by 51% ($p = .0083$ vs. young, t -test), while ISF Aβ₄₀ levels decreased by 20% ($p = .23$ vs. young, t -test). (B) Aβ₄₀/Aβ₄₂ ratio in the old mice is as much as 92% higher than in the young mice. ($p = .043$ vs. young, t -test). All data are presented as mean \pm SEM. Statistical significance was determined using the unpaired student t -test, n.s. not statistically significant ($p \geq .05$), * $p < .05$, ** $p < .005$.

to plaque formation, with memory deficits manifesting by 4 months as assessed by the radial arm maze and Morris water maze.^{51,53,54} Neuronal loss in J20 mice begins around 6 weeks, particularly in the CA1 region of the hippocampus.⁵¹ Epileptiform activities in APP transgenic mice manifest earlier than memory impairment or Aβ deposition.^{55–58} Hippocampal ISF samples before and after forming Aβ plaques were collected using *in vivo* microdialysis and then subjected to ELISA to determine the monomeric Aβ₄₀ and Aβ₄₂ levels, respectively. Soluble Aβ species, especially Aβ₄₂, reportedly decline in ISF as a result of their sequestration

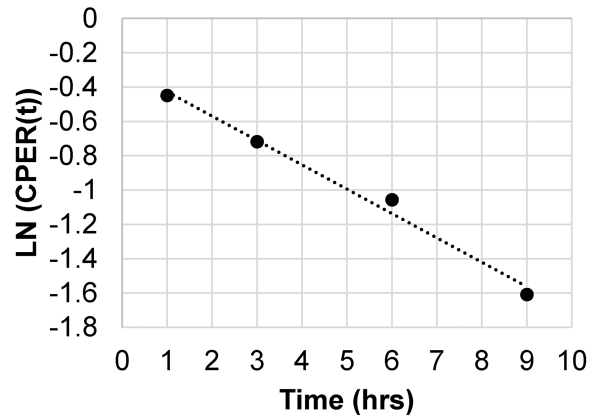
into amyloid plaques.⁵⁹ Consistently, the ISF Aβ₄₂ levels in 9–11-month-old J20 mice with Aβ deposition were significantly decreased by 51% as compared to 2–4-month-old J20 mice without Aβ deposition ($p = 0.0083$), whereas a difference in ISF Aβ₄₀ levels between the two groups was not statistically significant (Figure 1A). Indeed, the Aβ₄₀/Aβ₄₂ ratio was 92% higher in 9–11-month-old mice than in 2–4-month-old mice (Figure 1B). In the present study, therefore, we decided to use 2–4-month-old J20 mice without Aβ deposition as an appropriate model to evaluate the effect of PER on ISF Aβ metabolism before amyloid plaque formation.

FIGURE 2 A single oral administration of PER lowers ISF levels of Aβ₄₂ and Aβ₄₀ in a dose-dependent manner under sufficient plasma concentration. (A) 2 mg/kg or 5 mg/kg PER is orally administered to B6 mice ($n = 3$ per group) and 5 mg/kg PER to J20 mice ($n = 4$). The mean plasma concentrations of PER rapidly rise and maintain sufficient values for 9 h in B6 mice. Plasma concentrations at 1 or 5 h after the oral administration of PER (5 mg/kg) to J20 mice correspond to the plasma concentration profile obtained from the B6 mice. (B) Semi-log plot of mean plasma concentration of PER vs. time after 2 mg/kg administration to B6 mice ($n = 3$). The elimination of plasma PER follows first-order kinetics ($y = -0.14x - 0.29$, $R^2 = .99$). (C, D) Either 2 mg/kg PER, 5 mg/kg PER or vehicle is orally administered to 2–3-month-old J20 mice ($n = 10$ per group). ISF is collected every 1.5 h. The horizontal axis indicates the time since the treatment. For example, Aβ levels of ISF collected after oral administration up to 1.5 h are plotted at “0” h. ISF Aβ levels from 4.5 to 6 h after the treatment are shown in bar charts. ISF Aβ₄₀ levels declined rapidly after a PER administration in a dose-dependent manner ($p = .025$, two-way ANOVA for repeated measures, Bonferroni post hoc test). After 4.5 to 6 h of the PER treatment, the decrease in ISF Aβ₄₀ levels is 15% at 2 mg/kg and 20% at 5 mg/kg (C). ISF Aβ₄₂ levels declined rapidly after a PER administration in a dose-dependent manner ($p = .040$, two-way ANOVA for repeated measures, Bonferroni post hoc test). After 4.5 to 6 h of the PER treatment, the decrease in ISF Aβ₄₂ levels is 21% at the dose of 2 mg/kg and 31% at 5 mg/kg (D). (E) PER at the dose of 2 mg/kg or 5 mg/kg does not alter the ratio of ISF Aβ₄₀/Aβ₄₂ ($p = .41$, two-way ANOVA for repeated measures). All data are plotted as mean \pm SEM. n.s. denotes not statistically significant ($p \geq .05$), * $p < .05$.

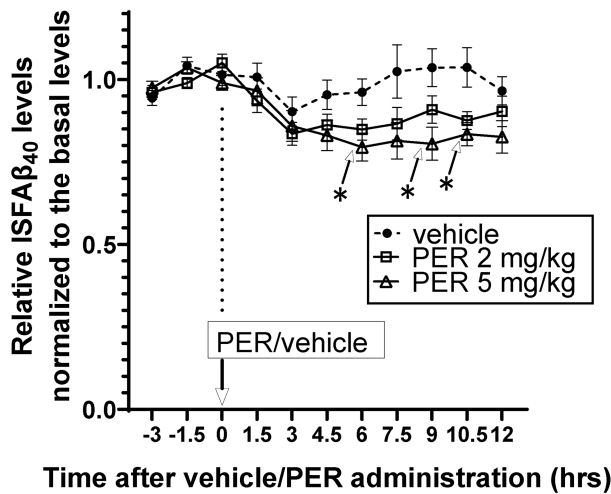
(A) The mean plasma concentration vs time after the oral administration of PER



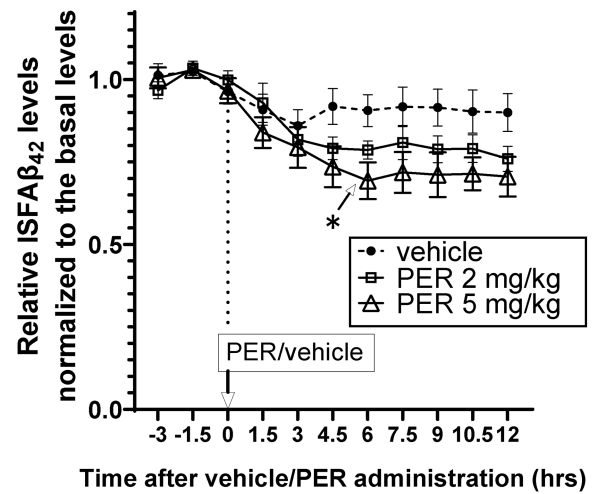
(B) Semi-log plot of mean plasma concentration of PER vs. time after 2 mg/kg administration (B6)



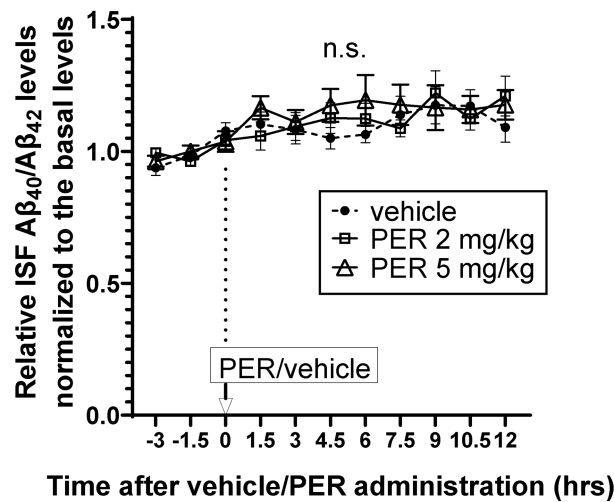
(C) ISF Aβ₄₀ levels



(D) ISF Aβ₄₂ levels



(E) Ratio of ISFAβ₄₀/Aβ₄₂ levels



3.2 | The plasma concentrations of PER rapidly rise and maintain sufficient values for 9 h after a single oral administration of PER

The half-life of PER after oral administration in mice has yet to be determined. We first assessed the plasma concentration of PER in B6 littermates to determine the kinetics of oral absorption of PER in mice after a single oral administration at doses of 2 and 5 mg/kg. The mean plasma concentration-time curve of PER in B6 mice is shown in Figure 2A. The peak levels were plotted at 1 h after 2 mg/kg PER administration (0.64 $\mu\text{g}/\text{mL}$) and at 3 h after 5 mg/kg PER administration (1.0 $\mu\text{g}/\text{mL}$) in B6 mice. The plasma levels decreased gradually from the peak and were as much as 0.48 $\mu\text{g}/\text{mL}$ at 9 h after 5 mg/kg treatment, compared with 0.20 $\mu\text{g}/\text{mL}$ after 2 mg/kg PER administration in B6 mice. According to a study in human patients, the mean serum PER concentration in patients who achieved $\geq 50\%$ reduction of seizure frequency was reported to be 0.450 $\mu\text{g}/\text{mL}$ (range: 0.085–1.5 $\mu\text{g}/\text{mL}$).⁶⁰ PER was reported to reduce excitatory postsynaptic field potentials with an IC_{50} of 0.23 μM (0.80 $\mu\text{g}/\text{mL}$) and an entire block at 3 μM (1 $\mu\text{g}/\text{mL}$) in mice, indicating that 2 or 5 mg/kg of PER should be a sufficient dose to regulate excessive neuronal activities. The elimination rate of PER in plasma followed first-order kinetics ($y = -0.14x - 0.29$, $R^2 = .99$). The half-life of PER in the plasma was 4.9 h (Figure 2B). The plasma levels in J20 mice after 5 mg/kg PER treatment were approximately consistent with the expected values in the case of B6 mice (1.03 $\mu\text{g}/\text{mL}$ at 1 h and 0.675 $\mu\text{g}/\text{mL}$ at 5 h). We thus concluded that the plasma concentration of PER in J20 mice displays a pattern similar to that in B6 mice (data not shown in the figure). Within 30 min after administering PER, all mice exhibited ataxia-like motor impairment. This condition gradually improved as the plasma levels of PER decreased.

3.3 | A single oral administration of PER lowers ISF levels of $\text{A}\beta_{42}$ as well as $\text{A}\beta_{40}$ in a dose-dependent manner

To evaluate the acute effect of the noncompetitive AMPAR inhibition on $\text{A}\beta$ metabolism, the ISF $\text{A}\beta_{40}$ and $\text{A}\beta_{42}$ levels

were assessed after a single oral administration of PER at doses of 2 and 5 mg/kg or vehicle ($n = 10$ in each group). All animals treated by PER at a dose of either 2 or 5 mg/kg rapidly exhibited mild motor impairment but they had gradually recovered in several hours. The motor effect seems to be necessary for the protective effects against aberrant neuronal activities because it has been reported that there was little or no separation between the PER doses that are effective in reducing seizures and doses causing motor impairment.³⁶ The ISF samples collected every 1.5 h before and after the treatment were subject to ELISA for $\text{A}\beta$ measurement. The $\text{A}\beta$ levels to the basal levels, an average of three-time points before the treatment, were plotted (Figure 2C,D).

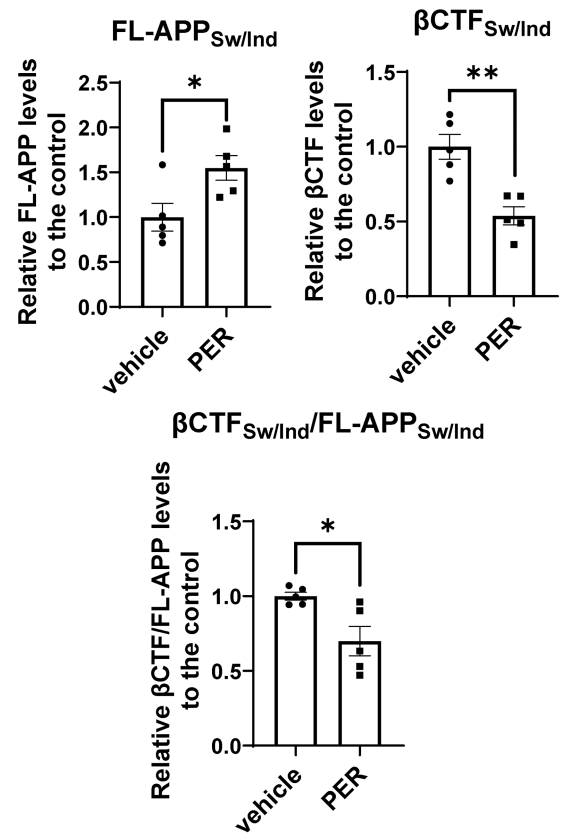
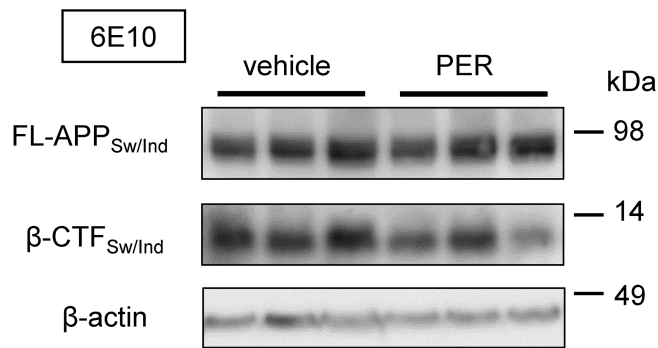
PER administration rapidly and significantly lowered both the ISF $\text{A}\beta_{40}$ and $\text{A}\beta_{42}$ levels in a dose-dependent manner, as compared with the vehicle. The ISF $\text{A}\beta_{40}$ levels were decreased by 15% at maximum after 4.5–6 h of 2 mg/kg PER administration, while a 20% decrement was seen following 5 mg/kg PER treatment (Figure 2C). A similar trend can be detected in the ISF $\text{A}\beta_{42}$ levels; ISF $\text{A}\beta_{42}$ levels were decreased by 21% and 31% after 4.5–6 h of 2 and 5 mg/kg PER treatments, respectively (Figure 2D). Next, to determine whether PER differently affects the metabolism of $\text{A}\beta_{40}$ and $\text{A}\beta_{42}$ in the ISF, we evaluated the ratio of ISF $\text{A}\beta_{40}$ to $\text{A}\beta_{42}$. As shown in Figure 2E, we observed no significant changes in the $\text{A}\beta_{40}/\text{A}\beta_{42}$ ratio before and after PER administration, suggesting that PER can regulate the ISF $\text{A}\beta$ levels.

3.4 | PER treatment significantly reduces the β -secretase-cleaved C-terminal fragments of $\text{APP}_{\text{Sw}/\text{Ind}}$ ($\beta\text{CTF}_{\text{Sw}/\text{Ind}}$) levels and increases the full-length $\text{APP}_{\text{Sw}/\text{Ind}}$ (FL- $\text{APP}_{\text{Sw}/\text{Ind}}$) levels

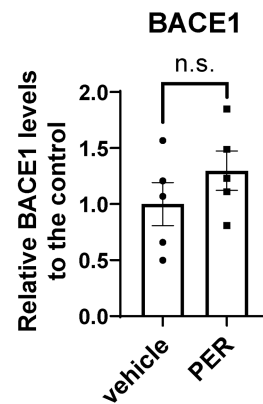
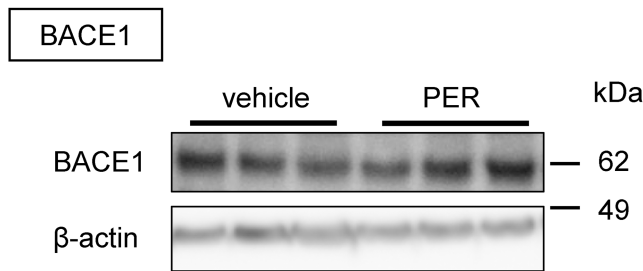
The ISF $\text{A}\beta$ levels should be determined by the balance of production, release into the extracellular milieu, and clearance from the ISF. To evaluate the effect of PER on amyloidogenic APP processing, we determined the FL- $\text{APP}_{\text{Sw}/\text{Ind}}$ and $\beta\text{CTF}_{\text{Sw}/\text{Ind}}$ levels in the hippocampal homogenates of J20 mice after the oral administration of either 5 mg/kg PER or vehicle by Western blotting (Figure 3A). We corrected the hippocampi at 5 h after

FIGURE 3 PER treatment significantly reduces the levels of β -secretase-cleaved C-terminal fragments of $\text{APP}_{\text{Sw}/\text{Ind}}$ ($\beta\text{CTF}_{\text{Sw}/\text{Ind}}$) and increases the full-length $\text{APP}_{\text{Sw}/\text{Ind}}$ (FL- $\text{APP}_{\text{Sw}/\text{Ind}}$) levels in the hippocampus. $\text{A}\beta$ levels in the hippocampus homogenates, intended to represent the hippocampal $\text{A}\beta$ pools excluding extracellular soluble $\text{A}\beta$, are determined by ELISA and remain unaffected by PER administration. (A) FL- $\text{APP}_{\text{Sw}/\text{Ind}}$ and $\beta\text{CTF}_{\text{Sw}/\text{Ind}}$ in the hippocampus are probed with 6E10 antibody. The $\beta\text{CTF}_{\text{Sw}/\text{Ind}}$ levels decrease by 46% in the PER group ($p = .0021$, t -test), while the FL- $\text{APP}_{\text{Sw}/\text{Ind}}$ levels increase by 55% ($p = .029$, t -test). Note that the ratio of $\beta\text{CTF}_{\text{Sw}/\text{Ind}}$ to FL- $\text{APP}_{\text{Sw}/\text{Ind}}$ is significantly decreased in the PER group ($p = .023$, t -test). (B) Total BACE1 levels in the hippocampus are unaffected by PER treatment ($p = .87$, t -test). (C) Neither $\text{A}\beta_{40}$ nor $\text{A}\beta_{42}$ levels in the hippocampal homogenates are affected by PER administration ($p = .52$, $.82$, t -test), and the ratio of $\text{A}\beta_{40}$ to $\text{A}\beta_{42}$ remains stable ($p = .23$). All data are plotted as mean \pm SEM. n.s. denotes not statistically significant ($p \geq .05$), * $p < .05$, ** $p < .005$.

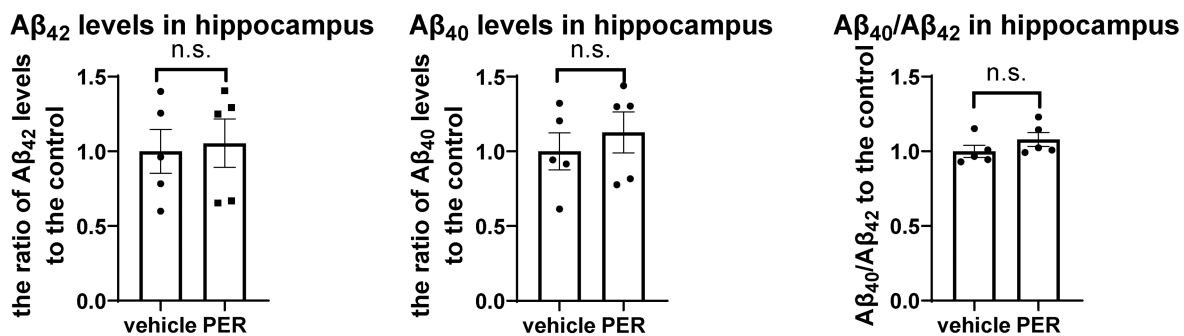
(A)



(B)



(C)



the administration because the ISF A β levels were estimated to decrease at most, as shown in Figure 2C,D. Western blotting analysis revealed that the levels of β -CTF_{Sw/Ind} were significantly decreased in the PER

group, while the FL-APP_{Sw/Ind} levels were increased (Figure 3A). Note that the ratio of β -CTF_{Sw/Ind} to FL-APP_{Sw/Ind} was significantly decreased in the PER group, indicating that acute treatment of PER clearly inhibits

β -cleavage of FL-APP_{Sw/Ind}, a preferable substrate for BACE1; meanwhile, the BACE1 levels were comparable between the vehicle and PER groups (Figure 3B). As shown in Figures 2C,D and 3A, our results suggest that acute treatment of PER reduces ISF A β levels in vivo through downregulation of β -cleavage rather than γ -cleavage in amyloidogenic processing.

3.5 | Acute administration of PER did not influence A β pools in the hippocampus, except for extracellular soluble A β

In the process of preparing the hippocampal homogenates, as detailed in the Materials and Methods section, hippocampi were sonicated in surfactant-free buffer. The pellets from the ultracentrifugation were then dissolved in RIPA buffer. As such, A β levels in the hippocampal homogenates should represent the entirety of hippocampal A β pools, excluding extracellular soluble A β . These homogenates were treated with 0.5M guanidine hydrochloride (Nacalai tesque, Kyoto, Japan), to facilitate the solubilization and monomerization of A β species. A β_{40} and A β_{42} levels were subsequently measured by ELISA. Notably, neither the levels of A β_{40} and A β_{42} nor their ratio in the hippocampal homogenates were affected by acute PER treatment (Figure 3C). This result indicates that the decline of ISF A β by PER is not due to their sequestration into other A β pools.

3.6 | PER administration does not affect the half-life of ISF A β levels

A β is derived from the sequential proteolytic cleavage of APP by β - and γ -secretases. To evaluate the alternation of A β clearance from ISF by PER treatment, the ISF samples were collected hourly using the in vivo microdialysis technique from the time of the subcutaneous injection of 3 mg/kg LY411575, a potent γ -secretase inhibitor (GSI), following oral administration of either 5 mg/kg PER or vehicle an hour earlier (Figure 4A). LY411575 can almost completely inhibit A β production, and we can only evaluate the A β clearance and estimate the ISF A β half-life periods by rapidly inhibiting A β production. The ISF A β_{40} levels were measured as a representative of A β species because the ISF A β_{40} levels after PER treatment showed similar kinetics with those of ISF A β_{42} . The ISF A β_{40} levels after the LY411575 injection are plotted in Figure 4B, and semi-log plot slopes are presented in Figure 4C. The

elimination of ISF A β_{40} followed first-order kinetics (vehicle: $y = -0.111x + 2.40$, $R^2 = 0.98$, PER: $y = -0.130x + 2.10$, $R^2 = .91$), and there was no significant change in the slopes of ISF between PER treatment and vehicle. The ISF A β_{40} elimination half-life calculated from the semi-log plot slope under PER treatment was approximately 2.3h, which was consistent with that under vehicle treatment (2.7h), indicating that the rapid decrement in ISF A β levels after the PER treatment was not due to enhanced clearance.

3.7 | Acute treatment of PER does not affect the levels of GluA1 and GluA2

AMPA receptors (AMPA receptors) are highly mobile and are transported to postsynapses in a structure- or neuronal activity-dependent manner, followed by recycling and degradation.⁶¹ AMPARs are heterotetramers composed of combinations of GluA1–GluA4 subunits, and GluA2, the determinant of Ca²⁺ permeation, is preferentially expressed in the adult brain.^{62,63} GluA1 is inserted at extrasynaptic sites and is potentiated at the synaptic surface in response to neuronal activity, whereas GluA2 structurally targets the synapses.^{64,65} Through the dynamics in the properties and abundance of synaptic AMPARs, functional changes, such as LTP and long-term depression (LTD), occur.^{66,67} To evaluate the effects of acute administration of PER on activity- or structure-dependent synaptic transport of AMPARs, we determined the GluA1 and GluA2 levels in SNS fractions by Western blotting. To first confirm the enrichment of synaptic proteins in the SNS fractions, the synaptotagmin 1 (Syt1) and postsynaptic density protein 95 (PSD95) levels in the THs and SNS fractions extracted from the cerebral cortex of J20 mice sacrificed at 5 h after vehicle administration were determined by Western blotting. The Syt1 and PSD95 levels were approximately 2.4-fold higher in the SNS fractions than in the THs, indicating sufficient enrichment of synaptic components in the SNS fractions (Figure 5A). Next, we determined the GluA1 and GluA2 levels in the SNS fractions and TH obtained from either vehicle or PER treatment mice by Western blotting. As shown in Figure 5B, the levels of GluA1 and GluA2 were not affected by PER administration, suggesting that PER did not downregulate the postsynaptic abundance of AMPARs, at least under the acute experimental condition. Since there is considerable variation in the levels of GluA1 and GluA2 in SNS and TH, the significance of the difference between PER and control cannot be fully dismissed.

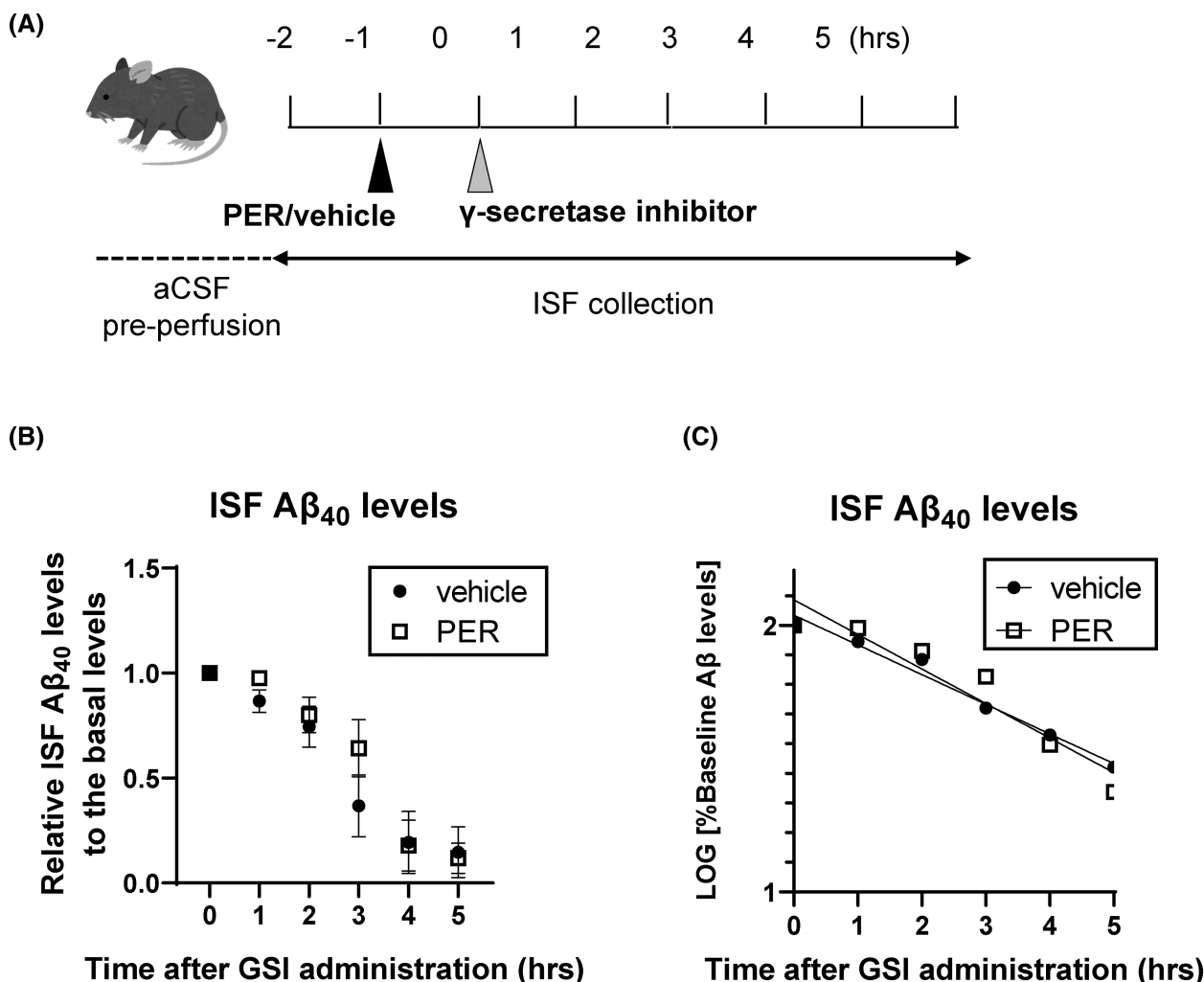


FIGURE 4 PER administration does not affect the half-life of ISF A β levels. (A) An experimental scheme to determine the elimination half-life of A β from ISF is shown. ISFs were collected every hour in J20 mice ($n=4$) before and after the oral administration of PER, followed by a subcutaneous injection of LY411575, a γ -secretase inhibitor (GSI), after 1 h. (B) ISF A β_{40} levels after GSI injection were plotted. (C) The half-life of A β_{40} was calculated from the slope of the ISF levels and time curve by plotting it on a semi-logarithmic graph. The elimination of ISF A β_{40} followed first-order kinetics (vehicle: $y = -0.111x + 2.40$, $R^2 = .98$, PER: $y = -0.130x + 2.10$, $R^2 = .91$), and there was no significant change in the slopes of ISF between the PER treatment and vehicle ($p = .46$, ANCOVA). The half-life was 2.3 h in PER treatment, almost the same as 2.7 h in the vehicle. All data are plotted as mean \pm SEM.

3.8 | PER treatment significantly reduces the levels of sAPP β released into the conditioned media of primary neuronal cultures under A β O-evoked neuronal hyperexcitability

To corroborate the above in vivo results showing that acute treatment of PER can suppress β -cleavage of APP under high A β O concentration, we applied primary neurons pre-incubated with A β O and TTX 24 h prior to co-treatment of glutamate with PER or vehicle to evoke neuronal hyperexcitability as a cellular in vitro AD model. The LDH levels released into the conditioned media did not display any significant differences between the PER and vehicle groups, indicating that PER treatment did not induce

significant cytotoxicity under the experimental condition (Figure 6A). We detected a significant reduction in the sAPP β levels released to the media in the PER group compared to vehicle group ($p = 0.037$), while the sAPP α levels remained unaltered between both (Figure 6B). To determine the levels of endogenous full-length APP (FL-APP) and APP-CTF, the total lysates were subjected to Western blotting with the APP C-terminal antibody. Consistent with the above in vivo results, the FL-APP levels were significantly higher in the PER group ($p = 0.0016$), whereas the α CTF levels were unchanged. Note that the blots of endogenous APP- β CTF could not be detected due to low expression levels. These findings suggest that PER treatment may suppress β -cleavage of APP in primary neurons exhibiting A β O-evoked neuronal hyperexcitability.

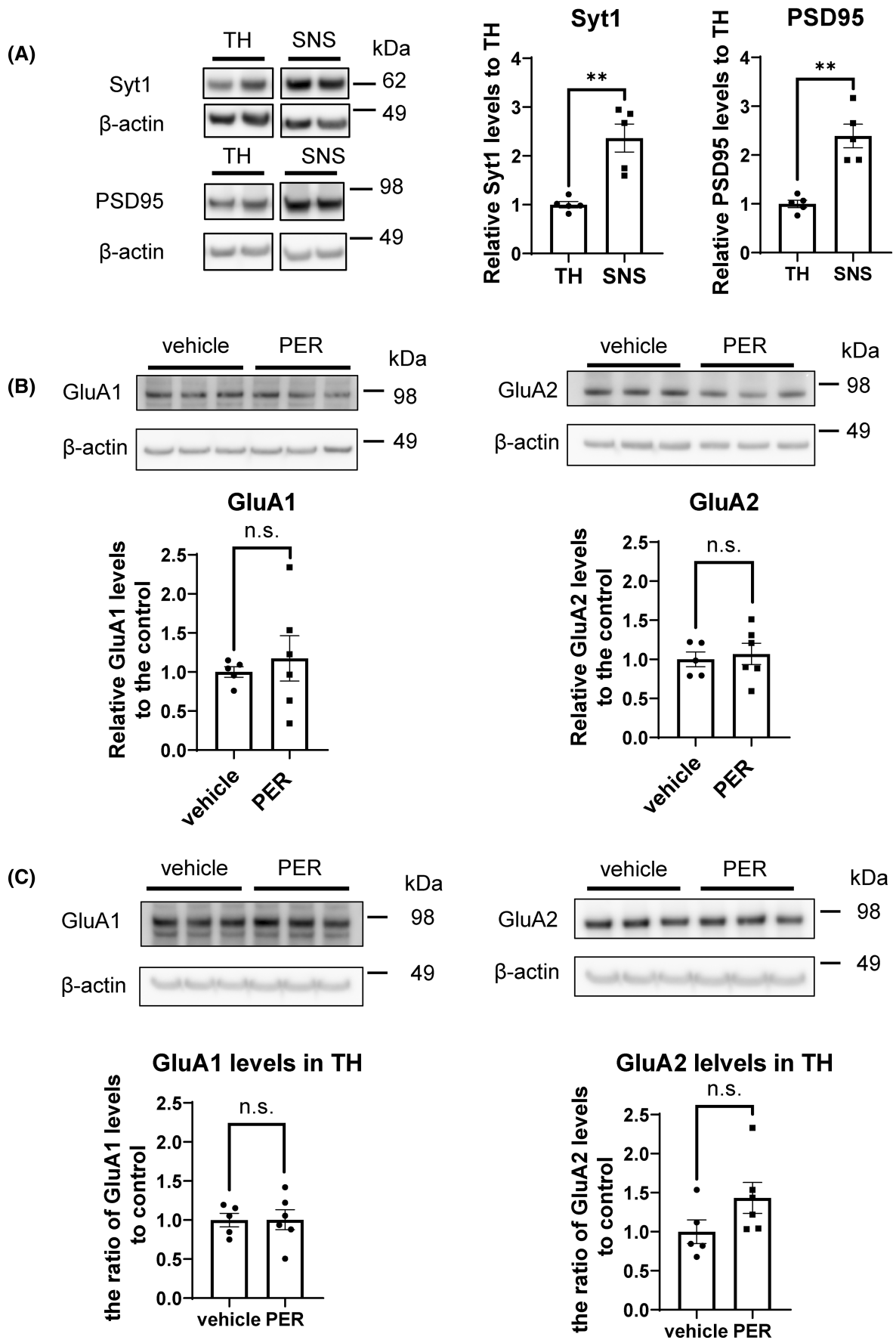


FIGURE 5 Acute treatment of PER does not affect the levels of GluA1 and GluA2. (A) Total homogenate (TH) and synaptoneuroosomes (SNS) of J20 hemicortex in the PER or vehicle-treated groups ($n=6$ and 5 , respectively) were electrophoresed in a single gel, and the lanes of synaptotagmin 1 (Syt1) and postsynaptic density protein 95 (PSD95) in the vehicle group were extracted. Syt1 levels were 2.4-fold higher in the SNS fraction than in total homogenates (TH) ($p < .0017$, t -test). Similarly, PSD95 levels were also 2.4-fold higher in the SNS fraction than in total homogenates ($p = .0006$, t -test). (B) No significant changes in the levels of GluA1 and GluA2 in SNS fractions and TH were observed between the vehicle and PER treatment ($p = .61$ and $.70$, respectively, t -test). All data are plotted as mean \pm SEM. n.s. denotes not statistically significant ($p \geq .05$), $**p < .005$.

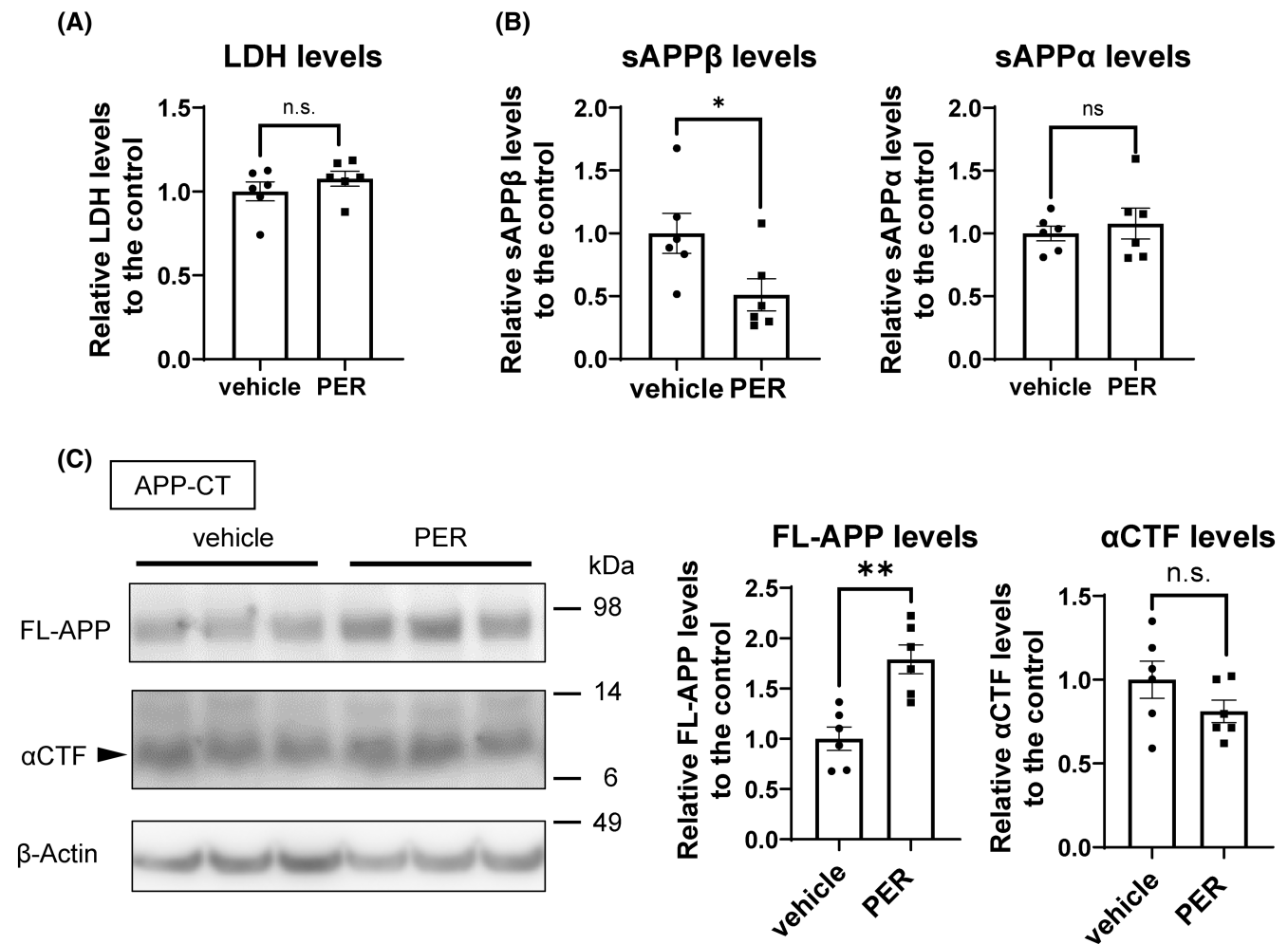


FIGURE 6 PER treatment significantly reduces the soluble APP β (sAPP β) levels in the medium and increases the full-length APP (FL-APP) levels in the lysates of primary neurons pretreated by TTX and A β O. (A) LDH levels in the medium were not affected by PER ($n=6$, $p = .67$, t -test). (B) sAPP β levels were decreased by 49% in the PER group ($n=6$, $p = .037$, t -test), while sAPP α levels tended to be increased but not significantly ($p = .068$, t -test). (C) FL-APP levels in the lysates were increased in the PER group by 79% ($n=6$, $p = .0016$, t -test). α CTF levels did not significantly change ($p = .18$, t -test). All data are plotted as mean \pm SEM. n.s. denotes not statistically significant ($p \geq .05$), $*p < .05$, $**p < .005$.

4 | DISCUSSION

Recent clinical research has demonstrated that comorbid epilepsy in AD, including subclinical seizures, can occur earlier than expected, even before the onset of cognitive impairment. Consistently, it has been previously reported that subclinical ictal activity and epileptic discharges are detected in EEG recordings before amyloid deposition in

a mouse model of AD.⁵⁵ Interestingly, using two-photon in vivo calcium imaging, Busche et al. revealed that “hyperactive” neurons indicated by increased intracellular calcium concentrations clustered near amyloid plaques and were very frequently detected even before A β deposition in the brains of APP Tg mice.^{58,68} Further, in a similar approach, local administration of a synthetic A β dimer supposed to be neurotoxic to the CA1 region of the

hippocampus in wild-type mice also induced hyperactive neurons.⁶⁹ Together, these findings suggest that A β pathology may directly induce neuronal hyperexcitability prior to A β deposition in the pathophysiology of AD. Based on the “neuronal hyperexcitability hypothesis” in AD, various antiepileptic drugs have been tested in AD model mice and AD patients. Sanchez et al. administered seven antiepileptic drugs (levetiracetam, ethosuximide, gabapentin, phenytoin, pregabalin, valproic acid, and vigabatrin) to APP Tg J20 mice before the appearance of A β deposition and found that only levetiracetam (LEV), which targets synaptic vesicle protein 2A (SV2A), showed a significant reduction in epileptic discharges, leading to improved synaptic transmission and cognitive function, whereas phenytoin and pregabalin significantly increased epileptic discharges.¹⁸

On the other hand, synapses have long been known to be one of the favorite sites for A β production, and it has been demonstrated *in vitro* and *in vivo* that A β is produced and released from synapses in an acute neuronal activity-dependent manner.^{70–74} Intriguingly, Yamamoto et al. reported that using an optogenetic approach, a long-term synaptic activation into the hippocampal perforant pathway originating from the lateral entorhinal cortex clearly promoted A β deposition in the projection area (the dentate gyrus) in APP Tg mice, suggesting that aberrant chronic synaptic activation accelerated A β burden. Further, in human studies, it has been shown that A β deposition starts in the brain regions in the default-mode network, which is considered to be highly active during rest,⁷⁵ and that A β deposition is more prominent in surgically resected brain sections from intractable epilepsy patients than age-matched controls.^{76,77} Based on a bidirectional association between A β pathology and epilepsy, we focused on a potential impact of AMPAR antagonist on A β pathology for the following reasons; (1) the expression levels of AMPAR^{78,79} and ISF glutamate levels⁸⁰ are concentrated at the epileptic foci even in interictal phases, (2) the levels of the GluA1 subunit to induce the Ca²⁺-permeable AMPA receptor is significantly increased in postsynaptic density-rich fractions from hippocampi of AD patients compared to controls⁸¹ injection of synthetic A β ₄₂ oligomers into rat hippocampal slice cultured neurons rapidly induced excitatory postsynaptic currents and increased the expression levels of synaptic Ca²⁺-permeable AMPA receptors.³¹

In the present study, we aimed to evaluate the therapeutic potential of PER targeting AMPAR toward A β pathology in AD. To this end, we investigated how PER affects A β pathology in J20 mice using *in vivo* microdialysis techniques. We found that a single oral administration of PER lowered ISF A β ₄₀ and A β ₄₂ levels (up to 21% and 31%, respectively) in the hippocampi of young J20 mice

without A β deposition. Acute administration of PER did not induce any alterations in A β pools within the hippocampus, except for extracellular soluble A β , suggesting that the reduction of ISF A β by a single administration of PER is not due to their sequestration into other A β pools. This result is in line with a previous study that highlighted how the ISF pools of A β collected using *in vivo* microdialysis reflect the regulation of A β metabolism.⁴⁶ In young APP mice without plaque formation, ISF A β pools should remain independent of other compartments, while in older mice with A β aggregation (plaques), insoluble A β could potentially contribute to changes in ISF A β levels, leading to an equilibrium between A β in ISF and deposited insoluble A β .

ISF soluble A β levels should be determined by balancing production and clearance from the ISF before A β aggregation starts. To evaluate the inhibitory effects of acute PER treatment on *in vivo* A β production, we assessed the APP substrates for β -secretase and γ -secretase to generate A β , FL-APP, and β CTF, respectively. We showed that 5 mg/kg PER treatment significantly reduced the levels of β CTF in hippocampal homogenates as well as the hippocampal ISF A β levels, indicating inhibited β -cleavage of APP. Indeed, we detected a significant reduction of sAPP β levels released from primary neurons under A β O-evoked neuronal hyperexcitability by acute treatment of PER, supporting the above *in vivo* findings. Regarding the A β clearance from ISF, the calculation of the half-life of ISF A β clarified that a single oral administration of PER did not alter the A β elimination from the hippocampal ISF. Another study that contradicts our results reported the positive effect of AMPAR activation on AD pathology: artificial activation of AMPARs can promote A β clearance.³⁴ We speculate that there may be an appropriate therapeutic window in which aberrant neural excitability is modified with little or no suppression of chronic AMPAR activation.

Since it has been shown that the appearance of regional A β deposition was preceded by an increase in soluble ISF A β levels in the corresponding regions of young APP Tg mice,^{46,82} a long-term modest reduction of soluble ISF A β could reduce future A β deposition under the pathogenic condition of AD.

We demonstrated for the first time that antagonism of AMPARs may reduce A β pathology by suppressing β -cleavage of APP in both *in vivo* and *in vitro* AD models. AMPARs are predominantly located at postsynapses, in contrast with the β -cleavage of APP, which mostly observed at presynapses.⁸³ Thus, PER is unlikely to directly affect BACE1; however, it might indirectly affect APP processing through neural activity modulation.

PER is already used clinically as an AED and an option in epilepsy complicated by AD. Our study

highlights PER as a therapeutic agent for AD, contrary to previous findings that AMPAR activation reduces A β pathology.^{34,84} This study has potential limitations in that we only examined the acute effects of a single oral administration.

In this study, all mice displayed ataxia-like motor impairment as the plasma concentration of PER reached sufficiently high levels. PER has been documented to induce dose-dependent motor incoordination in rodents, with a small therapeutic window.³⁵ However, PER rarely induces severe motor symptoms in human patients, potentially due to its longer half-life and the divergence in AMPAR distribution compared with rodents.³⁵ PER is associated with the occurrence of adverse events, including sleepiness, dizziness, motor symptoms, and psychiatric manifestations like irritability, anxiety, and aggressiveness.^{42,85–87} Patients with intellectual disabilities are more prone to psychological symptoms linked to PER.⁸⁸ Nevertheless, PER generally demonstrates favorable effectiveness and a robust safety profile in adult epilepsy patients, while in older patients, the occurrence of dizziness, fatigue, or balance disorders may be more frequent.^{42,43,85–87} Conversely, it has been indicated that there were no differences in the occurrence of behavioral and psychiatric adverse events according to the history of cognitive decline.⁴³ Furthermore, PER is well tolerated in patients aged ≥ 65 years, and low-dose PER has shown high efficacy in treating elderly-onset epilepsy concomitant with AD. Even conventional doses of PER have been observed to improve cognitive function, based on a limited study in Japan.⁴⁴ In a case report, PER improved both seizures and psychiatric symptoms in a patient with severe dementia who developed myoclonus epilepsy due to AD.⁸⁹ PER has also been reported to exert anxiolytic effects in mice via AMPAR antagonism.⁹⁰ Overall, the use of PER does not appear to increase the risk of psychiatric side effects in dementia patients, though the therapeutic window should be carefully determined considering background factors and pathological conditions.

In this study, we have highlighted the acute effect of PER on A β production, but neuronal hyperexcitability likely has multifactorial effects on AD pathophysiology. Aberrant neuronal excitability, such as epilepsy, itself affects cognitive function.⁹¹ Moreover, hyperexcitability should also contribute to the release and propagation of other pathogenic proteins, such as phosphorylated tau and α -synuclein.^{60,92–94} Other studies have shown that PER might also reduce inflammatory activation, tau-related excitotoxic synaptic signaling, and memory deficits in models with A β pathology, suggesting a broader impact of PER on AD pathophysiology.^{41,95} Further research with long-term administration and dose titration is needed to elucidate the multifactorial effects of PER in AD.

5 | CONCLUSIONS

A single oral administration of PER rapidly reduced ISF monomeric A β levels in the hippocampus of young J20 mice without altering A β clearance from ISF. Further, we found that acute treatment of PER reduced the β CTF levels in the hippocampi of APP Tg mice and the sAPP β levels secreted from the primary cortical neurons under A β -evoked neuronal hyperexcitability. Taken together, we concluded that the acute treatment of PER reduces A β production through suppressing β -cleavage of APP without altering synaptic AMPAR levels in both in vivo and in vitro AD models. This is the first report to reveal the inhibitory effect of PER on the amyloidogenic processing of APP.

AUTHOR CONTRIBUTIONS

Sakiho Ueda and Akira Kuzuya conceived and designed the research. Sakiho Ueda, Masayoshi Kawata, Kohei Okawa, Chika Honjo, Takafumi Wada, Mizuki Matsumoto and Kazuya Goto performed the research and acquired the data. Sakiho Ueda assembled the figures. All authors contributed to the analysis and interpretation of the data and were involved in drafting and revising the manuscript.

ACKNOWLEDGMENTS

We sincerely thank Prof. Takeshi Iwatsubo and Dr. Kaoru Yamada for allowing us to learn in vivo microdialysis techniques, Prof. Yukihiro Ohno for the valuable advice, and Eisai Co., Ltd. kindly offered PER. This work was supported in part by JSPS KAKENHI [grant number JP20K07884 (to A.K.)]; JSPS KAKENHI [grant number JP21K20690 (to S.U.)]; and the YOKOYAMA Foundation for Clinical Pharmacology (to S.U.).

DISCLOSURES

All authors declare that they have no conflicts of interest with the contents of this article.

DATA AVAILABILITY STATEMENT

The data that support the findings of this study are available in the methods of this article.

ORCID

Sakiho Ueda  <https://orcid.org/0000-0001-9198-0419>

Akira Kuzuya  <https://orcid.org/0009-0003-4925-9099>

Masayoshi Kawata  <https://orcid.org/0000-0003-4680-5376>

Kohei Okawa  <https://orcid.org/0009-0006-0634-7103>


Chika Honjo  <https://orcid.org/0009-0009-9724-4485>

Takafumi Wada  <https://orcid.org/0000-0002-6911-0609>

[org/0000-0002-6911-0609](https://orcid.org/0000-0002-6911-0609)

Mizuki Matsumoto  <https://orcid.org/0009-0005-4348-8928>

Kazuya Goto  <https://orcid.org/0000-0003-2235-3811>

Masakazu Miyamoto  <https://orcid.org/0000-0002-1370-0351>

Atsushi Yonezawa  <https://orcid.org/0000-0002-8057-6768>

Yasuto Tanabe  <https://orcid.org/0009-0002-0567-981X>

Akio Ikeda  <https://orcid.org/0000-0002-0790-2598>

Ayae Kinoshita  <https://orcid.org/0009-0000-9017-3754>

Ryosuke Takahashi  <https://orcid.org/0000-0002-1407-9640>

REFERENCES

- Masters CL, Simms G, Weinman NA, Multhaup G, McDonald BL, Beyreuther K. Amyloid plaque core protein in Alzheimer disease and Down syndrome. *Proc Natl Acad Sci.* 1985;82:4245-4249.
- Hardy J, Selkoe DJ. The amyloid hypothesis of Alzheimer's disease: progress and problems on the road to therapeutics. *Science.* 2002;297:353-356.
- Hardy JA, Higgins GA. Alzheimer's disease: the amyloid cascade hypothesis. *Science.* 1992;256:184-185.
- Sutphen CL, Jasielc MS, Shah AR, et al. Longitudinal cerebrospinal fluid biomarker changes in preclinical Alzheimer disease during middle age. *JAMA Neurol.* 2015;72:1029-1042.
- Jonsson T, Atwal JK, Steinberg S, et al. A mutation in APP protects against Alzheimer's disease and age-related cognitive decline. *Nature.* 2012;488:96-99.
- Sjogren T, Sjogren H, Lindgren AG. Morbus Alzheimer and morbus pick; a genetic, clinical and patho-anatomical study. *Acta Psychiatr Neurol Scand Suppl.* 1952;82:1-152.
- Förstl H, Burns A, Levy R, Cairns N, Luthert P, Lantos P. Neurologic signs in Alzheimer's disease: results of a prospective clinical and neuropathologic study. *Arch Neurol.* 1992;49:1038-1042.
- Mendez MF, Catanzaro P, Doss RC, Arguello R, Frey WH. Seizures in Alzheimer's disease: clinicopathologic study. *J Geriatr Psychiatry Neurol.* 1994;7:230-233.
- Mann DMA, Pickering-Brown SM, Takeuchi A, Iwatsubo T. Amyloid angiopathy and variability in amyloid β deposition is determined by mutation position in presenilin-1-linked Alzheimer's disease. *Am J Pathol.* 2001;158:2165-2175.
- Jayadev S, Leverenz JB, Steinbart E, et al. Alzheimer's disease phenotypes and genotypes associated with mutations in presenilin 2. *Brain.* 2010;133:1143-1154.
- Vossel KA, Beagle AJ, Rabinovici GD, et al. Seizures and epileptiform activity in the early stages of Alzheimer disease. *JAMA Neurol.* 2013;70:1158-1166.
- Vossel KA, Ranasinghe KG, Beagle AJ, et al. Incidence and impact of subclinical epileptiform activity in Alzheimer's disease. *Ann Neurol.* 2016;80:858-870.
- Lam AD, Deck G, Goldman A, Eskandar EN, Noebels J, Cole AJ. Silent hippocampal seizures and spikes identified by foramen ovale electrodes in Alzheimer's disease. *Nat Med.* 2017;23:678-680.
- Vossel K, Ranasinghe KG, Beagle AJ, et al. Effect of levetiracetam on cognition in patients with Alzheimer disease with and without epileptiform activity: a randomized clinical trial. *JAMA Neurol.* 2021;78:1345-1354.
- Bakker A, Albert MS, Krauss G, Speck CL, Gallagher M. Response of the medial temporal lobe network in amnesic mild cognitive impairment to therapeutic intervention assessed by fMRI and memory task performance. *NeuroImage: Clinical.* 2015;7:688-698.
- Bakker A, Krauss GL, Albert MS, et al. Reduction of hippocampal hyperactivity improves cognition in amnesic mild cognitive impairment. *Neuron.* 2012;74:467-474.
- Koh MT, Haberman RP, Foti S, McCown TJ, Gallagher M. Treatment strategies targeting excess hippocampal activity benefit aged rats with cognitive impairment. *Neuropsychopharmacology.* 2010;35:1016-1025.
- Sanchez PE, Zhu L, Verret L, et al. Levetiracetam suppresses neuronal network dysfunction and reverses synaptic and cognitive deficits in an Alzheimer's disease model. *Proc Natl Acad Sci.* 2012;109:E2895-E2903.
- Eddy CM, Rickards HE, Cavanna AE. The cognitive impact of antiepileptic drugs. *Ther Adv Neurol Disord.* 2011;4:385-407.
- Thompson P, Huppert FA, Trimble M. Phenytoin and cognitive function: effects on normal volunteers and implications for epilepsy. *Br J Clin Psychol.* 1981;20:155-162.
- Gallassi R, Morreale A, Lorusso S, Procaccianti G, Lugaresi E, Baruzzi A. Carbamazepine and phenytoin: comparison of cognitive effects in epileptic patients during monotherapy and withdrawal. *Arch Neurol.* 1988;45:892-894.
- Gallassi R, Morreale A, Di Sarro RA, Marra M, Lugaresi E, Baruzzi A. Cognitive effects of antiepileptic drug discontinuation. *Epilepsia.* 1992;33(suppl 6):S41-S44.
- Hessen E, Lossius MI, Reinvang I, Gjerstad L. Influence of major antiepileptic drugs on attention, reaction time, and speed of information processing: results from a randomized, double-blind, placebo-controlled withdrawal study of seizure-free epilepsy patients receiving monotherapy. *Epilepsia.* 2006;47:2038-2045.
- Park S-P, Kwon S-H. Cognitive effects of antiepileptic drugs. *J Cli Neurol (Seoul, Korea).* 2008;4:99-106.
- Taipale H, Gomm W, Broich K, et al. Use of antiepileptic drugs and dementia risk—an analysis of Finnish health register and German health insurance data. *J Am Geriatr Soc.* 2018;66:1123-1129.
- Li K-Y, Huang L-C, Chang Y-P, Yang Y-H. The effects of lacosamide on cognitive function and psychiatric profiles in patients with epilepsy. *Epilepsy Behav.* 2020;113:107580.
- Kauer JA, Malenka RC. Synaptic plasticity and addiction. *Nat Rev Neurosci.* 2007;8:844-858.
- Shankar GM, Li S, Mehta TH, et al. Amyloid- β protein dimers isolated directly from Alzheimer's brains impair synaptic plasticity and memory. *Nat Med.* 2008;14:837-842.
- Klyubin I, Walsh DM, Lemere CA, et al. Amyloid beta protein immunotherapy neutralizes Abeta oligomers that disrupt synaptic plasticity in vivo. *Nat Med.* 2005;11:556-561.
- Pellegrini-Giampietro DE, Gorter JA, Bennett MVL, Zukin RS. The GluR2 (GluR-B) hypothesis: Ca²⁺-permeable AMPA receptors in neurological disorders. *Trends Neurosci.* 1997;20:464-470.
- Whitcomb DJ, Hogg EL, Regan P, et al. Intracellular oligomeric amyloid-beta rapidly regulates GluA1 subunit of AMPA receptor in the hippocampus. *Sci Rep.* 2015;5:10934.

32. Wei-Qin Z, Francesca S, Robert B, et al. Inhibition of calcineurin-mediated endocytosis and alpha-amino-3-hydroxy-5-methyl-4-isoxazolepropionic acid (AMPA) receptors prevents amyloid beta oligomer-induced synaptic disruption. *J Biol Chem*. 2010;285(10):7619-7632.
33. Kim S, Ziff EB. Calcineurin mediates synaptic scaling via synaptic trafficking of Ca²⁺-permeable AMPA receptors. *PLoS Biol*. 2014;12:e1001900.
34. Hettinger JC, Lee H, Bu G, Holtzman DM, Cirrito JR. AMPA-ergic regulation of amyloid- β levels in an Alzheimer's disease mouse model. *Mol Neurodegenerat*. 2018;13:22.
35. Hanada T, Hashizume Y, Tokuhara N, et al. Perampanel: a novel, orally active, noncompetitive AMPA-receptor antagonist that reduces seizure activity in rodent models of epilepsy. *Epilepsia*. 2011;52:1331-1340.
36. Michael RA, Takahisa H. Preclinical pharmacology of perampanel, a selective non-competitive AMPA receptor antagonist. *Acta Neurol Scand*. 2013;127:19-24.
37. Carlson H, Ronne-Engström E, Ungerstedt U, Hillered L. Seizure related elevations of extracellular amino acids in human focal epilepsy. *Neurosci Lett*. 1992;140:30-32.
38. Matthew JD, Dennis DS. Extracellular hippocampal glutamate and spontaneous seizure in the conscious human brain. *Lancet (London, England)*. 1993;341(8861):1607-1610.
39. Cendes F, Andermann F, Carpenter S, Zatorre RJ, Cashman NR. Temporal lobe epilepsy caused by domoic acid intoxication: evidence for glutamate receptor-mediated excitotoxicity in humans. *Ann Neurol*. 1995;37:123-126.
40. Hanada T. Ionotropic glutamate receptors in epilepsy: a review focusing on AMPA and NMDA receptors. *Biomolecules*. 2020;10(3):464.
41. Bellingacci L, Tallarico M, Mancini A, et al. Non-competitive AMPA glutamate receptors antagonism by perampanel as a strategy to counteract hippocampal hyper-excitability and cognitive deficits in cerebral amyloidosis. *Neuropharmacology*. 2023;225:109373.
42. Inoue Y, Sumitomo K, Matsutani K, Ishii M. Evaluation of real-world effectiveness of perampanel in Japanese adults and older adults with epilepsy. *Epileptic Disord*. 2021;24:123-132.
43. Lattanzi S, Cagnetti C, Foschi N, et al. Adjunctive perampanel in older patients with epilepsy: a multicenter study of clinical practice. *Drugs Aging*. 2021;38:603-610.
44. Watanabe T, Osugi S, Soba T. Usefulness of long-term administration of perampanel in the treatment of elderly-onset epilepsy secondary to Alzheimer dementia. *J new Remedies Clin*. 2021;68:990-1003.
45. Gilbert J, Shu S, Yang X, Lu Y, Zhu L-Q, Man H-Y. β -Amyloid triggers aberrant over-scaling of homeostatic synaptic plasticity. *Acta Neuropathol Commun*. 2016;4:1-14.
46. Cirrito JR, May PC, O'Dell MA, et al. In vivo assessment of brain interstitial fluid with microdialysis reveals plaque-associated changes in amyloid-beta metabolism and half-life. *J Neurosci*. 2003;23:8844-8853.
47. Kuzuya A, Zoltowska KM, Post KL, et al. Identification of the novel activity-driven interaction between synaptotagmin 1 and presenilin 1 links calcium, synapse, and amyloid beta. *BMC Biol*. 2016;14:25.
48. Miyamoto M, Kuzuya A, Noda Y, et al. Synaptic vesicle protein 2B negatively regulates the Amyloidogenic processing of A β PP as a novel interaction partner of BACE1. *J Alzheimers Dis*. 2020;75:173-185.
49. Zhao T, Yu L-H, Zhang H-L, et al. Development and application of a novel LC-MS/MS method for human plasma concentration monitoring of perampanel in pediatric epilepsy patients. *Biomed Chromatogr*. 2022;36:e5446.
50. Mucke L, Masliah E, Yu GQ, et al. High-level neuronal expression of abeta 1-42 in wild-type human amyloid protein precursor transgenic mice: synaptotoxicity without plaque formation. *J Neurosci*. 2000;20:4050-4058.
51. Wright AL, Zinn R, Hohensinn B, et al. Neuroinflammation and neuronal loss precede A β plaque deposition in the hAPP-J20 mouse model of Alzheimer's disease. *PLoS ONE*. 2013;8:e59586.
52. Maesako M, Uemura K, Iwata A, et al. Continuation of exercise is necessary to inhibit high fat diet-induced β -amyloid deposition and memory deficit in amyloid precursor protein transgenic mice. *PLoS ONE*. 2013;8:e72796.
53. Cheng IH, Scarce-Levie K, Legleiter J, et al. Accelerating amyloid- β fibrillization reduces oligomer levels and functional deficits in Alzheimer disease mouse models. *J Biol Chem*. 2007;282:23818-23828.
54. Saganich MJ, Schroeder BE, Galvan V, Bredesen DE, Koo EH, Heinemann SF. Deficits in synaptic transmission and learning in amyloid precursor protein (APP) transgenic mice require C-terminal cleavage of APP. *J Neurosci*. 2006;26:13428-13436.
55. Palop JJ, Chin J, Roberson ED, et al. Aberrant excitatory neuronal activity and compensatory remodeling of inhibitory hippocampal circuits in mouse models of Alzheimer's disease. *Neuron*. 2007;55:697-711.
56. Bezzina C, Verret L, Juan C, et al. Early onset of hypersynchronous network activity and expression of a marker of chronic seizures in the Tg2576 mouse model of Alzheimer's disease. *PLoS ONE*. 2015;10:e0119910.
57. Kam K, Duffy Á, Moretto J, LaFrancois JJ, Scharfman HE. Interictal spikes during sleep are an early defect in the Tg2576 mouse model of β -amyloid neuropathology. *Sci Rep*. 2016;6:20119.
58. Busche MA, Chen X, Henning HA, et al. Critical role of soluble amyloid- β for early hippocampal hyperactivity in a mouse model of Alzheimer's disease. *Proc Natl Acad Sci*. 2012;109:8740-8745.
59. Hong S, Quintero-Monzon O, Ostaszewski BL, et al. Dynamic analysis of amyloid β -protein in behaving mice reveals opposing changes in ISF versus parenchymal A β during age-related plaque formation. *J Neurosci*. 2011;31:15861-15869.
60. Yamamoto Y, Usui N, Nishida T, et al. Therapeutic drug monitoring for Perampanel in Japanese epilepsy patients: influence of concomitant antiepileptic drugs. *Ther Drug Monit*. 2017;39:446-449.
61. Shi S-H. AMPA receptor dynamics and synaptic plasticity. *Science*. 2001;294:1851-1852.
62. Isaac JTR, Ashby MC, McBain CJ. The role of the GluR2 subunit in AMPA receptor function and synaptic plasticity. *Neuron*. 2007;54:859-871.
63. Lodge D. The history of the pharmacology and cloning of ionotropic glutamate receptors and the development of idiosyncratic nomenclature. *Neuropharmacology*. 2009;56:6-21.
64. Hayashi Y, Shi S-H, Esteban JA, Piccini A, Poncer J-C, Malinow R. Driving AMPA receptors into synapses by LTP and CaMKII:

- requirement for GluR1 and PDZ domain interaction. *Science*. 2000;287:2262-2267.
65. Passafaro M, Pièch V, Sheng M. Subunit-specific temporal and spatial patterns of AMPA receptor exocytosis in hippocampal neurons. *Nat Neurosci*. 2001;4:917-926.
 66. Granger AJ, Shi Y, Lu W, Cerpas M, Nicoll RA. LTP requires a reserve pool of glutamate receptors independent of subunit type. *Nature*. 2013;493:495-500.
 67. Buonarati OR, Hammes EA, Watson JF, Greger IH, Hell JW. Mechanisms of postsynaptic localization of AMPA-type glutamate receptors and their regulation during long-term potentiation. *Sci Signal*. 2019;12:eaar6889.
 68. Busche MA, Eichhoff G, Adelsberger H, et al. Clusters of hyperactive neurons near amyloid plaques in a mouse model of Alzheimer's disease. *Science*. 2008;321:1686-1689.
 69. Zott B, Simon MM, Hong W, et al. A vicious cycle of β amyloid-dependent neuronal hyperactivation. *Science*. 2019;365:559-565.
 70. Kamenetz F, Tomita T, Hsieh H, et al. APP processing and synaptic function. *Neuron*. 2003;37:925-937.
 71. Lesné S, Ali C, Gabriel C, et al. NMDA receptor activation inhibits alpha-secretase and promotes neuronal amyloid-beta production. *J Neurosci*. 2005;25:9367-9377.
 72. Cirrito JR, Yamada KA, Finn MB, et al. Synaptic activity regulates interstitial fluid amyloid-beta levels in vivo. *Neuron*. 2005;48:913-922.
 73. Cirrito JR, Kang JE, Lee J, et al. Endocytosis is required for synaptic activity-dependent release of amyloid-beta in vivo. *Neuron*. 2008;58:42-51.
 74. Hoe H-S, Fu Z, Makarova A, et al. The effects of amyloid precursor protein on postsynaptic composition and activity. *J Biol Chem*. 2009;284:8495-8506.
 75. Buckner RL, Snyder AZ, Shannon BJ, et al. Molecular, structural, and functional characterization of Alzheimer's disease: evidence for a relationship between default activity, amyloid, and memory. *J Neurosci*. 2005;25:7709-7717.
 76. Mackenzie IRA, McLachlan RS, Kubu CS, Miller LA. Prospective neuropsychological assessment of nondemented patients with biopsy proven senile plaques. *Neurology*. 1996;46:425-429.
 77. Gourmaud S, Shou H, Irwin DJ, et al. Alzheimer-like amyloid and tau alterations associated with cognitive deficit in temporal lobe epilepsy. *Brain*. 2020;143:191-209.
 78. Zilles K, Qü MS, Köhling R, Speckmann EJ. Iontropic glutamate and GABA receptors in human epileptic neocortical tissue: quantitative in vitro receptor autoradiography. *Neuroscience*. 1999;94:1051-1061.
 79. Graebnitz S, Kedo O, Speckmann E-J, et al. Interictal-like network activity and receptor expression in the epileptic human lateral amygdala. *Brain*. 2011;134:2929-2947.
 80. Çavuş I, Romanyshyn JC, Kennard JT, et al. Elevated basal glutamate and unchanged glutamine and GABA in refractory epilepsy: microdialysis study of 79 patients at the yale epilepsy surgery program. *Ann Neurol*. 2016;80:35-45.
 81. Marcello E, Epis R, Saraceno C, et al. SAP97-mediated local trafficking is altered in Alzheimer disease patients' hippocampus. *Neurobiol Aging*. 2012;33:422.e1.
 82. Bero AW, Yan P, Roh JH, et al. Neuronal activity regulates the regional vulnerability to amyloid- β deposition. *Nat Neurosci*. 2011;14:750-756.
 83. Del Prete D, Lombino F, Liu X, D'Adamio L. APP is cleaved by Bace1 in pre-synaptic vesicles and establishes a pre-synaptic Interactome, via its intracellular domain, with molecular complexes that regulate pre-synaptic vesicles functions. *PLoS One*. 2014;9:e108576.
 84. Hoey SE, Buonocore F, Cox CJ, Hammond VJ, Perkinton MS, Williams RJ. AMPA receptor activation promotes non-amyloidogenic amyloid precursor protein processing and suppresses neuronal amyloid- β production. *PLoS One*. 2013;8:e78155.
 85. Toledano Delgado R, García-Morales I, Parejo-Carbonell B, et al. Effectiveness and safety of perampanel monotherapy for focal and generalized tonic-clonic seizures: experience from a national multicenter registry. *Epilepsia*. 2020;61:1109-1119.
 86. Leppik IE, Wechsler RT, Williams B, Yang H, Zhou S, Laurenza A. Efficacy and safety of perampanel in the subgroup of elderly patients included in the phase III epilepsy clinical trials. *Epilepsy Res*. 2015;110:216-220.
 87. Liguori C, Izzi F, Manfredi N, et al. Efficacy and tolerability of perampanel and levetiracetam as first add-on therapy in patients with epilepsy: a retrospective single center study. *Epilepsy Behav*. 2018;80:173-176.
 88. Snoeijs-Schouwenaars FM, van Ool JS, Tan IY, Schelhaas HJ, Majoie MHJM. Evaluation of perampanel in patients with intellectual disability and epilepsy. *Epilepsy Behav*. 2017;66:64-67.
 89. Kumamoto A, Chiba Y, Suda A, Hishimoto A, Kase A. A severe dementia case in end of life care with psychiatric symptoms treated by perampanel. *J Epilepsy Res*. 2021;11:93-95.
 90. Bektas N, Arslan R, Alyu F. The anxiolytic effect of perampanel and possible mechanisms mediating its anxiolytic effect in mice. *Life Sci*. 2020;261:118359.
 91. Helmstaedter C, Witt J-A. Epilepsy and cognition—a bidirectional relationship? *Seizure-Eur J Epilep*. 2017;49:83-89.
 92. Yamada K, Iwatsubo T. Extracellular α -synuclein levels are regulated by neuronal activity. *Mol Neurodegenerat*. 2018;13:9.
 93. Ueda J, Uemura N, Sawamura M, et al. Perampanel inhibits α -Synuclein transmission in Parkinson's disease models. *Mov Disord*. 2021;36:1554-1564.
 94. Yamada K, Holth JK, Liao F, et al. Neuronal activity regulates extracellular tau in vivo. *J Exp Med*. 2014;211:387-393.
 95. Monteiro-Fernandes D, Silva JM, Soares-Cunha C, et al. Allosteric modulation of AMPA receptors counteracts Tau-related excitotoxic synaptic signaling and memory deficits in stress- and A β -evoked hippocampal pathology. *Mol Psychiatry*. 2021;26:5899-5911.

How to cite this article: Ueda S, Kuzuya A, Kawata M, et al. Acute inhibition of AMPA receptors by perampanel reduces amyloid β -protein levels by suppressing β -cleavage of APP in Alzheimer's disease models. *The FASEB Journal*. 2023;37:e23252. doi:[10.1096/fj.202300837R](https://doi.org/10.1096/fj.202300837R)